1040-5488/03/8001-0036/0 VOL. 80, NO. 1, PP. 36–42
OPTOMETRY AND VISION SCIENCE


ORIGINAL ARTICLE

# A Method to Predict Refractive Errors from Wave Aberration Data

**ANTONIO GUIRAO, PhD and DAVID R. WILLIAMS, PhD**

*Laboratorio de Óptica, Departamento de Física, Universidad de Murcia, Campus de Espinardo Murcia, Spain (AG), Center for Visual Science, University of Rochester, River Campus, Rochester, New York (DRW)*

**ABSTRACT: We explored the impact of the eye's higher-order aberrations on subjective refraction comparing two classes of methods for estimating refractive state, one based directly on the wave aberration defined in the pupil plane and another based on the retinal image plane. The method defined in the pupil plane chose the sphere and cylinder that either minimized the wave aberration root mean square or minimized the sum of all the spherical and cylindrical components in the wave aberration. The method defined in the image plane chose the sphere and cylinder that optimized an image-quality metric such as the Strehl intensity ratio, the entropy and the intensity variance of the point-spread function, the volume under the modulation transfer function, or the volume under the contrast-sensitivity function. All these methods were compared in a population of six eyes for which we measured both the wave aberration with a Shack-Hartmann wavefront sensor and the subjective refraction under identical conditions. Pupil plane methods predicted subjective refraction poorly. The mean absolute error of the prediction, in spherical equivalent, was about 0.5 D (range, 0.1 to 0.8 D) and increased with increases in higher-order aberrations. However, for all the retinal image plane methods, the mean error between predicted and subjective refraction was about 0.1 D (range, 0 to 0.25 D). The reliability of the method based on the image-quality optimization was further confirmed in a large population of 146 eyes. In conclusion, higher-order aberrations influence the amount of sphere and cylinder required to correct vision. The results indicate that subjective refraction can be predicted from the eye's optics alone by optimizing computed retinal image quality. (Optom Vis Sci 2003;80:36–42)**

Key Words: aberrations, subjective refraction, objective refraction, refractive errors, image-quality metrics, retinal image quality

A number of objective techniques (retinoscopy, autorefraction, and photorefraction) can be used to measure the spherical and cylindrical refractive errors of the human eye. Because they are much faster than subjective refraction, they are attractive alternatives to performing a subjective refraction. Objective refraction is not only useful but often essential, for example, when examining young children and patients with mental or language difficulties. However, a major concern is whether these objective methods correctly estimate the best subjective refraction of the observer. The limitations of autorefractors in accuracy and repeatability are well known. For example, there are discrepancies between autorefractive and subjective measurements,[1] especially with astigmatism[2] or when the degree of ametropia is large.[3] In general, patients prefer the clinician subjective refraction to autorefraction.[4] Also, retinoscopy and autorefraction usually disagree to some extent.[5] The eye has higher-order aberrations beyond defocus and astigmatism,[6–12] and one possible reason for the lack of agreement between subjective and objective methods is that some objective methods may not properly take higher-order aberrations into account. For example, it has been shown that there can be a significant degree of uncertainty in photorefraction measurements when the spherical aberration of the eye is considered.[13] Aberrations also influence the retinoscopic measure.[14] An increase with age of the error between subjective refraction and autorefraction has been found,[15] which could arise from the fact that higher-order aberrations increase with age.[16, 17] Some autorefractors may somehow incorporate the effect of higher-order aberrations by, for example, maximizing the contrast of a target imaged on the retina. However, it is more often the case that they base their estimate on a smaller pupil size than is used in the subjective refraction, which underestimates the role of higher-order aberrations.

Thus, there is a need to develop an objective method to estimate refraction that takes into account the effect of the eye's higher-order aberrations. These aberrations can now be measured quickly, accurately, and repetitively, for instance, with a Shack-Hartmann sensor.[18] This paper addresses the question of how to compute the

subjective refraction from these wave aberration measurements. Such a method would be useful, not only for prescribing spectacles and contact lenses, but especially for refining refractive surgery, where the possibility to re-treat an eye is limited.

In this article, we describe a procedure that calculates the combination of sphere and cylinder that optimizes different image-quality metrics based on the distribution of light in the computed retinal image. The method yields an optimum image that is correlated with the subjective best retinal image. Experimental results are presented that compare the subjective refraction in a population of subjects with the objective refraction showing the reliability and accuracy of the method.

## Higher-Order Aberrations and the Eye's Refraction Pupil Plane Metrics

The diagrams in Fig. 1 show an example of the image formation by a myopic eye with and without higher-order aberrations. Without aberrations (Fig. 1a), all the rays would focus on the paraxial plane, and then the refraction of the eye would be calculated from the spherical negative lens required to displace the focal plane to the plane lying on the retina. However, due to aberrations (Fig. 1b), the rays passing through the edge of the pupil converge at a focus that is not coincident or even coaxial with the paraxial focus. This simple example shows how the distribution of rays in different planes produces images with different quality. The refraction of that eye should be the one required for displacing a plane of "best image" to the retina. Two well-known simple cases are the case of the least confusion plane for an astigmatic eye corrected only for defocus and the case of the extra focus required to best correct an eye that has spherical aberration. Similarly, other higher-order aberrations also play a role, affecting not only the focus correction but the correction of astigmatism as well. Thus, the best image is not necessarily achieved by correcting the defocus and astigmatism corresponding to the paraxial approximation, which neglects the effects of higher-order aberrations. A pertinent question is what constitutes a "best image." From geometric ray tracing, the answer is that the best image would correspond to a plane where the size of the spot is at a minimum. However, the spots determined geometrically do not accurately reflect the point-spread function (PSF), which must be calculated based on the aberrated wavefront and the diffraction of the light at the exit pupil. The distribution of light in the actual optical image is usually very different from the image predicted geometrically.

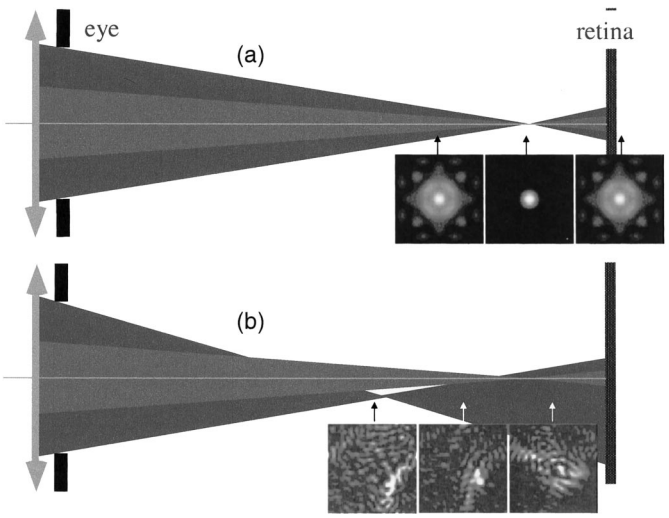


**FIGURE 1.**

a: Schematic of a myopic eye with no higher-order aberrations, and distributions of light at the paraxial plane and at both sides of it. b: Myopic eye with higher-order aberrations. In this case, the images do not have a symmetrical distribution.

Another candidate for the best image plane is the plane where the root mean square (RMS) of the wave aberrations is minimum. The higher-order aberrations may be combined with lower-order aberrations, which is known as "balancing." One of the main properties of the popular Zernike polynomials is that they represent balanced aberrations. Second-order polynomials, $Z_2^{0,\pm 2}$, represent defocus and astigmatism. For instance, spherical aberration is balanced with defocus in the Zernike term $Z_4^0$; the terms $Z_4^{\pm 2}$ are balanced with astigmatism, etc. The aberration balancing may lead one to assume incorrectly that a minimum RMS of the aberrated wavefront produces the best image. Hence, the RMS of the wave aberration is commonly used as a measure of how aberrated an eye is. A fact that has supported that use is that the RMS correlates, for small aberrations, with another popular metric also used as a criterion of image quality, the Strehl intensity ratio, defined as the ratio of the peak irradiance in the PSF to the peak irradiance in a diffraction-limited system. A large value of Strehl ratio indicates good image quality. For small aberrations, Strehl ratio and RMS of the wave aberration are inversely proportional: when the Strehl ratio is maximum, the RMS is minimum. Several equations have been derived to express this relationship[19]; one of the best known is

$$S = \exp\left[ -\left(\frac{2\pi}{\lambda}\mathrm{RMS}\right)^2 \right] \quad (1)$$

where S is the Strehl ratio and $\lambda$ is the wavelength. The eye's wave aberration is usually decomposed in the variance-normalized Zernike base after being measured:

$$\mathrm{WA} = \sum_{n,m} c_n^m Z_n^m \quad (2)$$

(See Thibos et al.[20] for the double-index Zernike coefficient ordering). An advantage of that is that the RMS of the wave aberration can then be obtained easily from the Zernike coefficients as

$$\mathrm{RMS}^2 = \sum_{n,m} (c_n^m)^2 \quad (3)$$

Thus, any correction of the refractive errors of the eye could be determined by setting to zero the corresponding Zernike coefficients: $c_2^{0,\pm 2} = 0$. But, again, the image analysis based on diffraction of the wavefront shows the failure in general of that idea. When aberrations are large, a maximum in Strehl ratio can be obtained with nonoptimally balanced aberrations[21, 22] (i.e., not a minimum in the RMS). More concretely, when the RMS of the wave aberration is larger than about 0.15 wavelengths, Equation 1 is no longer valid. In comparison, the value for example of the spherical aberration of the normal average eye is 2 to 4 wavelengths for a pupil diameter of 6 mm. Thus, the sphere and cylinder required to prescribe refraction and achieve the best image quality can not be obtained in general from the assumption of minimum RMS.

We have discussed above two possible methods to estimate the refraction of the eye from wave aberration data. In the paraxial approximation, one extracts the total defocus and astigmatism from the wave aberration. By minimizing the RMS, one uses the values of balanced defocus and astigmatism. However, any consideration about image quality should be done using diffraction analysis. In the next section, we describe a superior method to obtain the eye's refraction by calculating the optimum image quality given the wave aberration of the eye.

## Optimization Procedure and Image-Quality Metrics

Our computational procedure calculates the refraction based on the optimum value of an image-quality metric that describes retinal image quality. The procedure executes a search in a three-dimensional space, finding the values of sphere, cylinder, and axis of the correcting lens that give the optimum value of the metric.

Let $WA_{eye}$ be the wave aberration of the eye, in Zernike polynomials:

$$\mathrm{WA_{eye}} = c_2^0 Z_2^0 + c_2^2 Z_2^2 + c^{-2}{}_2 Z^{-2}{}_2 + \mathrm{WA_{higher\ order}} \qquad (4)$$

where $Z_n^m$ are the Zernike polynomials and $c_n^m$, the Zernike coefficients. Let $WA_{lens}$ be the wave aberration of the prescribed lens that corrects the eye's defocus and astigmatism:

$$\mathrm{WA_{lens}} = a_2^0 Z_2^0 + a_2^2 Z_2^2 + a^{-2}{}_2 Z^{-2}{}_2 \qquad (5)$$

The wave aberration of the corrected eye will be

$$\mathrm{WA_{eye}} + \mathrm{WA_{lens}} = b_2^0 Z_2^0 + b_2^2 Z_2^2 + b^{-2}{}_2 Z^{-2}{}_2 + \mathrm{WA_{higher\ orders}} \qquad (6)$$

where $b_2^0 = c_2^0 + a_2^0$, $b_2^2 = c_2^2 + a_2^2$, and $b^{-2}{}_2 = c^{-2}{}_2 + a^{-2}{}_2$. The image-quality metric computed from this wave aberration must be optimum.

We tested several image-quality metrics, some of them in the spatial domain based on the PSF and others in the Fourier domain based on the modulation transfer function (MTF). The PSF may be interpreted as the retinal image of a point source. The more compact the PSF, the better the retinal image quality. The MTF characterizes the ability of the eye to form sharp images of a grating. The higher the MTF, the higher the contrast in the image of the grating. Below is the description of the different metrics (see Fig. 2 for a schematic).

## In the Spatial Domain of the PSF

*The Strehl Ratio, or Peak Value of the Normalized PSF.* The generalized pupil function, *P*, is first calculated as

$$P = p \times \exp[i(2\pi/\lambda)(\mathrm{WA_{lens}} + \mathrm{WA_{eye}})] \qquad (7)$$

where *p* denotes a circular pupil aperture with a unit amplitude function. The PSF is calculated as the squared modulus of the Fourier transform of the generalized pupil function:

$$\mathrm{PSF} = |\mathrm{FT}(P)|^2 \qquad (8)$$

We did not consider the Stiles-Crawford effect, but this can be incorporated into the pupil function by using a Gaussian model for the pupil aperture, *p*. In any case, we have previously verified that the Stiles-Crawford effect is practically negligible in the computed PSF.

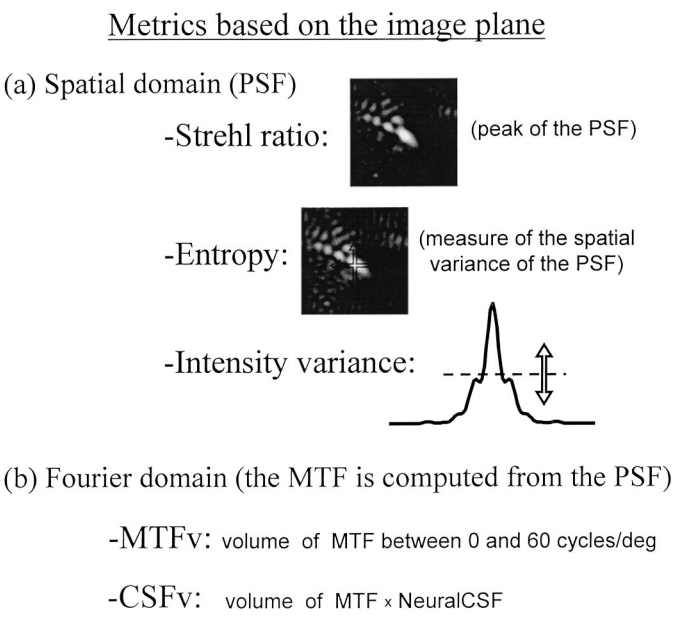


**FIGURE 2.**
Schematic of the different image-quality metrics for the optimization method.

*The Entropy of the PSF.* The entropy is mathematically calculated as follows:

$$\mathrm{entropy} = -\sum_{x,y} \mathrm{PSF}(x, y) \times \log \mathrm{PSF}(x, y) \qquad (9)$$

where *(x,y)* indicates the position (pixels) and *log* is the decimal logarithm. This metric is a measure of the spatial variance of the PSF, i.e., a measure of how the energy is distributed in the image. The aberration-free PSF has the minimum entropy. Aberrations increase the entropy.[23]

*The Intensity Variance of the PSF.* The intensity variance of the PSF is calculated as the average value of squared PSF minus the average PSF squared:

$$\mathrm{var(PSF)} = \overline{\mathrm{PSF}^2} - \mathrm{PSF}^2 \qquad (10)$$

## In the Fourier Domain

*The Volume of the MTF between 0 and 60 cpd.* The MTF is the modulus of the Fourier transform of the PSF (alternatively the autocorrelation of the generalized pupil function):

$$\mathrm{MTF} = |\mathrm{FT(PSF)}| \qquad (11)$$

*The Volume of the Contrast Sensitivity Function (CSF).* The CSF is calculated as the product of the optical MTF and the neural contrast sensitivity function,[24] NCSF:

$$\mathrm{CSF}(f_x, f_y) = \mathrm{MTF}(f_x, f_y) \times \mathrm{NCSF}(f_x, f_y) \qquad (12)$$

The independent variables for the three-dimensional search were the coefficients $b_2^0$, $b_2^2$, and $b_2{}^{-2}$. The starting point was de-

termined by the criterion of minimum RMS of the WA (i.e., $b_2^0 = b_2^2 = b_2^{-2} = 0$), not by the subjective refraction. To avoid local maxima we used an exhaustive method of search of the tridimensional space. The search ran in steps of the parameters $b_2^0$, $b_2^2$, and $b_2^{-2}$ that corresponded to 0.05 D and 5° for the axis. The extremes of the search intervals were chosen far enough apart to ensure that the maxima identified were global maxima.

The derivation of the sphere and cylinder from the Zernike coefficients that made optimum the image-quality metric will now be described. The $WA_{lens}$ in the Seidel form is

$$WA_{lens}(\rho, \theta) = A_d\rho^2 + A_a\rho^2 \cos(\theta - \theta_a) \quad (13)$$

where $\rho$ is the normalized radial distance from the axis, $\theta$ is the azimuthal angle in the pupil, and $\theta_a$ indicates the axis of the astigmatism. The sphere ($S$) and cylinder ($C$), in D, of the correcting lens is

$$S = -\frac{2}{r_o^2}A_d\,,\ C = -\frac{2}{r_o^2}A_a \quad (14)$$

where $r_0$ is the radius of the pupil that the WA describes. We have the following relationship between Zernike coefficients and Seidel coefficients:

$$A_a = 2\sqrt{6}\sqrt{(a_2^2)^2 + (a_2^{-2})^2}\,,\ A_d = 2\sqrt{3}a_2^0 - A_a/2 \quad (15)$$

with the axis given by $\theta_a = 1/2\arctan a_2^{-2}/a_2^2$. The Zernike coefficients for the lens are obtained from the coefficients of the eye's WA and the coefficients yielded by the search $a_2^{0,\pm 2} = b_2^{0,\pm 2} - c_2^{0,\pm 2}$.

## Experiment

To find out whether a metric performs better than the others, we carried out an experiment consisting of measuring the subjective refractions in a sample of eyes and comparing them with the objective refractions calculated from the wave aberration data. See Fig. 3 for a schematic of the experiment.

## METHODS

Measurements were obtained in six normal young subjects. Subjects were selected after an ophthalmological examination that confirmed no pathology and normal visual acuity. Subjects ranged in age from 23 to 35 years (mean ± SD, 29 ± 4 years). Refractive errors ranged from −1.75 to −4 D for sphere (−3.3 ± 0.8 D), and from 0 to −1 for astigmatism (−0.6 ± 0.4 D). The eye's pupil was dilated and the accommodation paralyzed by instilling two drops of cyclopentolate 1%, 5 min between drops. The study followed the tenets of the Declaration of Helsinki, and signed informed consent was obtained from the every subject after explanation of the nature and possible consequences of the study.

We measured the wave aberrations with a Shack-Hartmann wavefront sensor[25] (221 lenslets, lenslet spacing = 0.4 mm, and focal length = 24 mm). A 790-nm infrared superluminescent diode serves as a beacon, forming a point source on the retina. Light reflected from the retina emerges through the eye's pupil as an aberrated wavefront. The eye's pupil is conjugate with the lenslet array of the sensor, which forms the Shack-Hartmann image. From that image, the wave aberration is determined. An artificial pupil of 6 mm in diameter was used. We measured the aberrations for a 6-mm-diameter pupil to the sixth radial order (28 Zernike coefficients). The error corresponding to axial chromatic aberration from 790 to 570 nm was added to the term of defocus in the wave aberration.

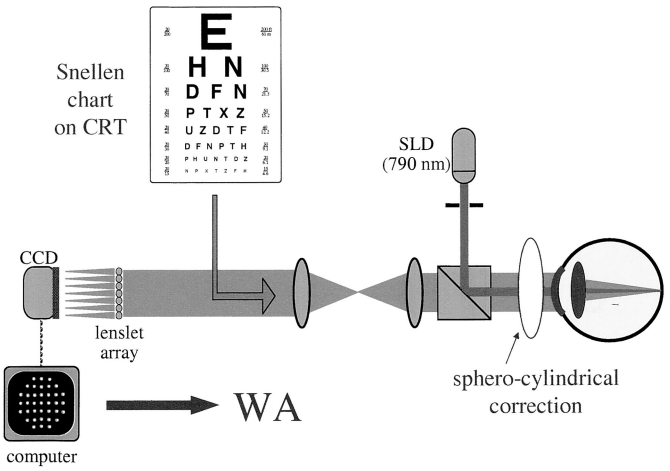


**FIGURE 3.**
Schematic of the experiment performed in six eyes to determine whether the image-quality metric optimization is adequate to estimate subjective refraction. An infrared superluminescent diode (SLD) serves as a beacon, forming a point source on the retina. Light from the retina emerges through the eye's pupil as an aberrated wavefront. The eye's pupil is conjugate with the lenslet array of a Shack-Hartmann sensor, which forms the Shack-Hartmann image. From that image, the wave aberration is determined. The subjective refraction is measured by projecting a Snellen chart through the system for the same experimental conditions. The refractive error is corrected with spherocylindrical lenses before measuring the wave aberration.

To obtain the subjective refraction, the best vision sphere was first determined with a Snellen chart at 6 ft. Then the astigmatism was measured by means of a fan chart and the fogging method. This first estimation of the refraction was then refined by means of a Snellen chart displayed on a cathode ray tube that the subject viewed through the optics of the experimental system with the 6-mm pupil. The end-point criterion for determining the final subjective refraction consisted of achieving the maximum visual acuity. The spherical and cylindrical power adjustments were made in step sizes of 0.25 D. The subjective refraction was always monocular.

After the subjective refraction, the determined correction was kept in front of the eye by means of spherocylindrical trial lenses. Thus, the measured wave aberration is that of the eye plus that of the correcting lens. If the correct metric is used, the wave aberrations measured in those conditions should directly yield a computed image quality that is optimum or close to the optimum because the eye's aberrations are measured after the correction of defocus and astigmatism. Any possible aberrations in the trial lenses are taken into account with this experimental procedure.

## RESULTS

Fig. 4 shows the average error from the six eyes between the subjective and the objective refraction (in spherical equivalent), for the five image-quality metrics and for the two pupil plane metrics.

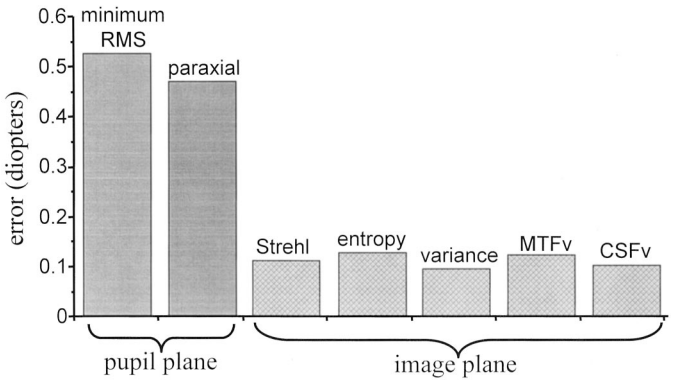


**FIGURE 4.**

Average error across six eyes between subjective and objective refraction. Objective refraction was calculated by using two pupil plane methods (paraxial approximation and minimum root mean square [RMS]) and by optimizing five different image-quality metrics.

On average, the error when one uses the methods based on the pupil plane (either, the minimum RMS criterion or the paraxial approximation) was about 0.5 D (range, 0.1 to 0.8 D). By optimizing the image-quality metrics, the error between subjective and objective refraction was 0.1 ± 0.08 D (range, 0 to 0.25 D). This error was lower than the smallest step size (0.25 D) typically used in prescribing spectacles and contact lenses. There was no significance difference between the five image-quality metrics.

For the pupil plane methods, the error estimating the subjective refraction is dependent on the eye's higher-order aberrations. Fig. 5 shows the error for each eye between the subjective and the objective refraction, estimated by means of the two pupil plane methods, as a function of the RMS of the wave aberration of each eye (without including defocus and astigmatism). The error increases when the amount of higher-order aberrations increases. This is expected for the method based on the paraxial approximation because it directly neglects the effect of higher-order aberrations. But we also see that the minimum RMS is not a good indicator of the best image quality. This is because the method based on the minimum RMS criterion takes into account the higher-order aberrations in the pupil plane, not in the image plane, and the mathematical transformation (based on Fourier transforms) from one plane to the other often produces results that are not intuitive.

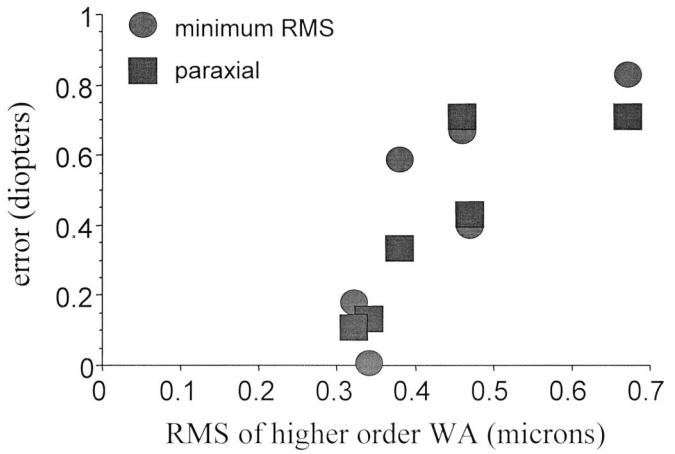


**FIGURE 5.**

Error between subjective and objective refraction in each of six eyes for the two pupil plane methods, as a function of the root mean square (RMS) of the wave aberration of each eye (including only higher-order aberrations).

*Test of the Method in a Large Population of Eyes.* To test further the reliability of the method, we compared the objective refraction calculated by image-quality optimization and the subjective refraction in a large population of subjects. We used the wave aberration data previously measured[12] in a population of 146 eyes from 73 normal subjects. Subjects ranged in age from 24 to 66 years (mean, 45 ± 10). The aberrations were measured with a Shack-Hartmann sensor for a pupil 5.7 mm in diameter to the fifth radial order with natural accommodation. The Shack-Hartmann sensor had a total of 57 lenslets (spacing = 0.6 mm and focal length = 40 mm). Aberrations were measured at 780 nm. The clinical subjective refraction was available for each eye. This refraction was binocular. Refractive errors ranged from −10.75 to 4.25 D for sphere (mean, −3 ± 3 D), and from 0 to −4.25 for astigmatism (mean, −0.5 ± 0.75 D).

Fig. 6a shows the correlation between subjective spherical equivalent (sphere plus half the cylinder) and the objective spherical equivalent calculated by metric optimization. (The results shown are for the optimization of the Strehl ratio, but there was no significant difference for the other metrics.) The correlation coefficient was close to one ($r^2 = 0.98$). The average error across the 146 eyes between subjective and objective refraction in spherical equivalent was 0.4 ± 0.5 D. Fig. 6b shows the correlation between the subjective and the objective cylinder ($r^2 = 0.87$). The average error in the estimated cylinder was 0.2 ± 0.3 D. Fig. 6c shows the same correlation for the axis of the cylinder ($r^2 = 0.89$). The errors for the whole population were <1 D for sphere and <0.5 D for cylinder.

Fig. 7 shows the error between subjective and objective refraction as a function of the eye's aberrations. Fig. 7 a and c correspond to the estimation of objective refraction by using pupil plane methods, and Fig. 7 b and d correspond to the optimization method using image-quality metrics. When the pupil plane methods are used, both the spherical equivalent and the cylinder show systematic errors that correlate with the higher-order aberrations. With image-quality optimization, there is no correlation between the error in the refraction and the aberrations.

## DISCUSSION

We showed how the amount of sphere and cylinder required to correct vision is different from both the amount that minimizes the

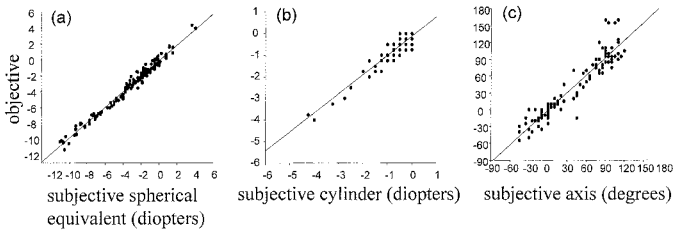


**FIGURE 6.**

Correlation between the clinical subjective refraction and the objective refraction in a population of 146 eyes for the spherical equivalent (a), for the cylinder (b), and for the axis of the cylinder (c). The objective refraction was obtained by image-quality metric optimization.

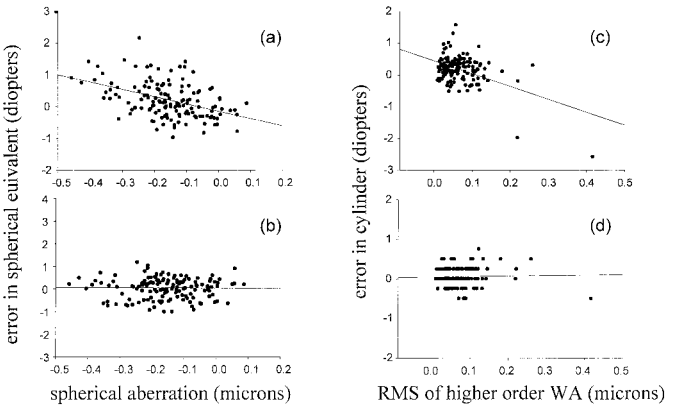


**FIGURE 7.**

Correlation with higher-order aberrations of the error between subjective and objective refraction in 146 eyes for pupil plane methods (a, c) and for image-quality metric optimization (b, d). a, b: the error in spherical equivalent; c, d: the error in cylinder.

RMS of the wave aberration and the total amount in the wave aberration. Thus, methods that use the coefficients of the wave aberration (i.e., based on the pupil plane) fail in predicting the eye's refraction. The error in the prediction increases when the amount of higher-order aberrations increases, indicating the need to consider the role of higher-order aberrations. Although the minimum wave aberration RMS criterion involves balanced aberrations, we have shown that it is not the best metric for the typical amounts of aberrations in the human eye.

On the other hand, we have proposed an objective method based on the optimization of retinal image quality and demonstrated that it performs well in predicting the subjective refraction of the eye. The experiment performed on six subjects showed that the error between predicted and subjective refraction can be as low as 0.1 D when the subjective and the objective refraction are obtained under identical experimental conditions. In the large population of 146 eyes, we found excellent correlation between subjective and objective refraction, either for sphere, cylinder, or axis. There is, however, some variability with the average error between subjective and objective refraction being 0.4 D for sphere and 0.2 D for cylinder. We attribute these larger errors to several factors. First, it should be noted that the wave aberrations were measured in this large population with natural accommodation and for a 5.7-mm pupil. Although a fixation target was used, small fluctuations of the accommodation may increase the experimental error. It is also likely that subjective refractions were performed for pupil sizes other than 5.7 mm. Another possible factor could be that whereas the WA measurements took into account the possible aberrations of the correcting lenses in the sample of six subjects, this was not the case in the measurements of the aberrations in the large population. Finally, whereas the subjective refraction was monocular and the end-point criterion consisted of reaching the maximum visual acuity (comparable with a maximum in the metric) in the prospective study in six eyes, in the large population, the refraction was binocular and the end-point criterion likely was not the maximum visual acuity but perhaps consisted of reaching the 20/20 line.

Although vision performance ultimately depends on the combination of optical and retinal and neural factors, it seems from our results that the optimization of the retinal image taking into account only the optics of the eye is an accurate method to predict the refractive errors of the eye. In other words, the best objective image quality closely corresponds to the best subjective image quality in terms of refraction. It is important to note that the vision task that we have evaluated is the subjective refraction based on the subjective quality and recognition of letters. However, the present results do not guarantee that retinal image optimization will correlate with the best performance for other visual tasks.

A goal of our study was to find an adequate metric that describes image quality and allows us, by means of its optimization, to predict the subjective refraction. We tested a number of these metrics both in the spatial and in the Fourier domain and found no significant difference between them. It has sometimes been debated whether the Strehl ratio is a good indicator of image quality for the eye. When the Strehl ratio falls to low levels, the extent and the shape of the PSF could become more important than its peak value.[26] In addition, any increases in the Strehl ratio associated with optimization of spatial frequencies in the MTF above 60 cpd would not be relevant for vision because of the limitations of receptoral and neural factors.[27] Finally, the PSF may have several peaks that would make a metric based on the Strehl ratio ambiguous. It happens, however, that for the distribution of aberrations of the human eye, the MTF is very small above 60 cpd, so both the Strehl ratio and the volume of the MTF are robust metrics. Additionally, the similarity of using the volume of the CSF or the volume of the MTF indicates no significant effect of the neural transfer function on the best subjective refraction. With respect to the intensity variance of the PSF, the larger the variance, the sharper the PSF. The entropy of the PSF is a measure of the spatial variance or spread of the PSF. The lower the entropy, the more compact and sharper the PSF. Thus, the correlation between Strehl ratio, variance, and entropy is expected. Although not presented here, we also tested as an image-quality metric the encircled energy that falls within an area corresponding to the Airy disk. The results were similar to those with the other metrics. In sum, we proposed several image-quality metrics, which must be optimized to find the refraction of the subject, and found that all of them correlated well and are equally reliable. It seems likely that additional experiments with greater statistical power will be able to distinguish between these metrics. Additional experiments that involve a wider variety of visual stimuli and an assessment of subjective image quality rather than merely optimizing it may reveal interesting differences between image-quality metrics. Nonetheless, it is of some interest that if differences do exist, they are not large enough to affect this particular task.

As a practical application, wavefront sensors that capture the complete wave aberration of the eye can improve objective refraction by using image plane metrics to incorporate the effect of higher-order aberrations. One of the advantages of refracting the eye from wavefront sensing instead of an autorefractor is that the refraction can be computed for any desired pupil size. Wavefront sensors provide the complete information on the optics of the eye and can tailor the prescription for the patient's pupil size. The cost in time of performing metric optimization is not large. Commercial computers of about 1 GHz can make the PSF and image metric calculations in 1 to 10 s (depending on the amount of aberrations).

The optimization of an image-quality metric allows not only an estimation of the subjective refraction, but also a simulation of scenes that the subject would see after a best correction of defocus and astigmatism. Of course, there are retinal and neural factors that will ultimately affect the perceptual experience of the observer.

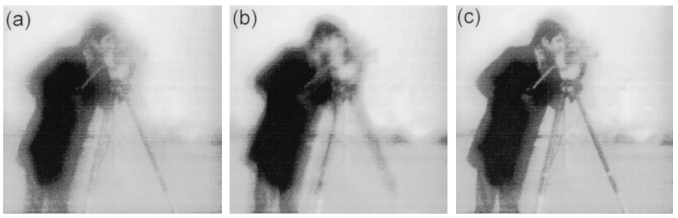


**FIGURE 8.**
Simulated images of a scene as it would be viewed by correcting a normal eye with the refraction calculated with the pupil plane methods: minimum root mean square (RMS) (a) and paraxial approximation (b) and with the prescription obtained with the image-quality optimization (c).

However, these computational simulations provide at least an estimation of what will optimize vision as well as a view of how much vision improves when the refractive errors of the eye are corrected. In Fig. 8, there is a series of simulated images in white light after correcting a typical eye with the refraction calculated with the pupil plane methods (Fig. 8 a and b) and with the prescription obtained with the image-quality optimization (Fig. 8c). The comparison of the three images shows that the optimization of image-plane metrics produces the least blurred image.

## ACKNOWLEDGMENTS

*This work was supported in part by National Eye Institute, National Institutes of Health grants EY04367 and EY01319. A. Guirao was supported, in part, by a postdoctoral fellowship from Ministerio de Educación y Cultura (Spain).*

*Part of the results of this manuscript were presented as a paper at the Optical Society of America Annual Meeting, October 2000, Providence, RI, and at a meeting of the Association for Research in Vision and Ophthalmology, May 2001, Fort Lauderdale, FL.*

*Received April 10, 2002; revision received September 30, 2002.*

## REFERENCES

1. Elliott M, Simpson T, Richter D, Fonn D. Repeatability and accuracy of automated refraction: a comparison of the Nikon NRK-8000, the Nidek AR-1000, and subjective refraction. Optom Vis Sci 1997; 74:434–8.
2. Walline JJ, Kinney KA, Zadnik K, Mutti DO. Repeatability and validity of astigmatism measurements. J Refract Surg 1999;15: 23–31.
3. Thompson AM, Li T, Peck LB, Howland HC, Counts R, Bobier WR. Accuracy and precision of the Tomey ViVA infrared photorefractor. Optom Vis Sci 1996;73:644–52.
4. Bullimore MA, Fusaro RE, Adams CW. The repeatability of automated and clinician refraction. Optom Vis Sci 1998;75:617–22.
5. Harvey EM, Miller JM, Dobson V, Tyszko R, Davis AL. Measurement of refractive error in Native American preschoolers: validity and reproducibility of autorefraction. Optom Vis Sci 2000;77:140–9.
6. Smirnov MS. Measurement of the wave aberration of the human eye. Biophysics 1962;7:766–95.
7. Howland HC, Howland B. A subjective method for the measurement of monochromatic aberrations of the eye. J Opt Soc Am 1977;67: 1508–18.
8. Walsh G, Charman WN, Howland HC. Objective technique for the determination of monochromatic aberrations of the human eye. J Opt Soc Am (A) 1984;1:987–92.
9. Artal P, Marcos S, Navarro R, Williams DR. Odd aberrations and double-pass measurements of retinal image quality. J Opt Soc Am (A) 1995;12:195–201.
10. Liang J, Williams DR. Aberrations and retinal image quality of the normal human eye. J Opt Soc Am (A) 1997;14:2873–83.
11. He JC, Marcos S, Webb RH, Burns SA. Measurement of the wavefront aberration of the eye by a fast psychophysical procedure. J Opt Soc Am (A) 1998;15:2449–56.
12. Porter J, Guirao A, Cox IG, Williams DR. Monochromatic aberrations of the human eye in a large population. J Opt Soc Am (A) 2001;18:1793–803.
13. Campbell MC, Bobier WR, Roorda A. Effect of monochromatic aberrations on photorefractive patterns. J Opt Soc Am (A) 1995;12: 1637–46.
14. Roorda A, Bobier WR. Geometrical technique to determine the influence of monochromatic aberrations on retinoscopy. J Opt Soc Am (A)1996;13:3–11.
15. Joubert L, Harris WF. Excess of autorefraction over subjective refraction: dependence on age. Optom Vis Sci 1997;74:439–44.
16. Guirao A, Gonzalez C, Redondo M, Geraghty E, Norrby S, Artal P. Average optical performance of the human eye as a function of age in a normal population. Invest Ophthalmol Vis Sci 1999;40:203–13.
17. Artal P, Berrio E, Guirao A, Piers P. Contribution of the cornea and internal surfaces to the change of ocular aberrations with age. J Opt Soc Am (A) 2002;19:137–43.
18. Liang J, Williams DR. Aberrations and retinal image quality of the normal human eye. J Opt Soc Am (A) 1997;14:2873–83.
19. Mahajan VN. Strehl ratio for primary aberrations: some analytical results for circular and annular pupils. J Opt Soc Am 1982;72: 1258–66.
20. Thibos LN, Applegate RA, Schwiegerling JT, Webb R. Standards for reporting the optical aberrations of eyes. In: Lakshminarayanan V, ed. Trends in Optics and Photonics. Vision Science and Its Applications, Vol 35. OSA Technical Digest Series. Washington, DC: Optical Society of America, 2000:232–44.
21. King WB. Dependence of the Strehl ratio on the magnitude of the variance of the wave aberration. J Opt Soc Am 1968;58:655–61.
22. Mahajan VN. Aberration Theory Made Simple. Bellingham, WA: SPIE Press, 1991.
23. Barakat R. Some entropic aspects of optical diffraction imagery. Optics Commun 1998;156:235–9.
24. Williams DR. Visibility of interference fringes near the resolution limit. J Opt Soc Am (A)1985;2:1087–93.
25. Liang J, Williams DR. Aberrations and retinal image quality of the normal human eye. J Opt Soc Am (A) 1997;14:2873–83.
26. Mouroulis P, Zhang HP. Visual instrument image quality metrics and the effects of coma and astigmatism. J Opt Soc Am (A) 1992;9: 34–42.
27. Williams DR. Aliasing in human foveal vision. Vision Res 1985;25: 195–205.

**Antonio Guirao**
*Laboratorio de Óptica*
*Departamento de Física*
*Universidad de Murcia*
*Campus de Espinardo (Edificio C)*
*30071 Murcia*
*Spain*
*e-mail: aguirao@um.es*